Acta Crystallographica Section B
Structural Science
ISSN 0108-7681

Synthesis and structure of, and bonding in some derivatives of 2,6,9,10-tetraoxatricyclo[3.3.1.1^{3,8}]-decane

J. Simons,[a] H. G. Thomas,[a] S. R. Hall[b] and G. Raabe[b]*†

[a]Institut für Organische Chemie, Rheinisch-Westfälische Technische Hochschule Aachen, Prof.-Pirlet-Strasse 1, D-52074 Aachen, Germany, and [b]Crystallography Centre, University of Western Australia, Nedlands, Western Australia 6009, Australia

† Permanent address: Institut für Organische Chemie, Rheinisch-Westfälische Technische Hochschule Aachen, Prof.-Pirlet-Strasse 1, D-52074 Aachen, Germany.

Correspondence e-mail: gerd.raabe@thc.rwth-aachen.de

Received 19 May 2000
Accepted 27 September 2000

Five derivatives of 2,6,9,10-tetraoxatricyclo[3.3.1.1^{3,8}]decane were synthesized and their molecular structures in the solid state were determined by means of X-ray diffraction analysis. In addition, the structures of all the molecules were optimized at different levels of computational quantum chemistry (HF/6-31G*, B3LYP/6-31G*). Experimentally determined bond lengths were compared with their calculated counterparts, and striking differences between the *Hartree–Fock* (HF) results and the experimental data could be traced back to the lack of correlation energy in the geometry optimizations. Two of the compounds under consideration are diastereomers and their relative stability was not only calculated with a conventional *ab initio* method (ZPE+MP2/6-31G*//HF/6-31G*), but also within the framework of density functional theory (B3LYP/6-31G*). In some of the calculations the influence of the solvent was included in single point calculations by means of an electrostatic model. Moreover, combining experimental as well as computational results, the exclusive axial orientation of a Cl atom in one of the compounds could be explained by an interplay of kinetic and energetic effects.

1. Introduction

In previous publications (Thomas *et al.*, 1993; Simons, 1992) we not only described the electrochemical synthesis, but also the reactivity of some substituted 4,7,8-trioxabicyclo[3.2.1]oct-2-enes [(2), Scheme (I)].

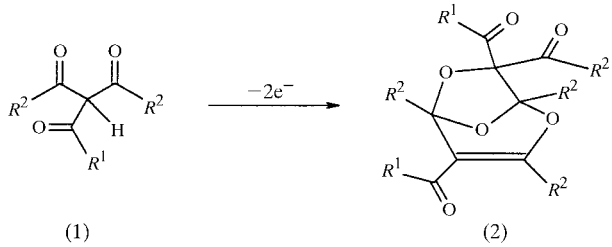

(1)
(*a*) $R^1 = R^2 = CH_3$
(*b*) $R^1 = OCH_3$; $R^2 = CH_3$

(2)
(*a*) $R^1 = R^2 = CH_3$
(*b*) $R^1 = OCH_3$; $R^2 = CH_3$

(I)

The molecular structures of some of the reaction products described in these reports are not easily accessible by means of standard spectroscopic tools. We therefore now report on their structures as determined by means of X-ray diffraction methods.

Other questions which remained unanswered so far concern the relative yields of two diastereomeric compounds and the highly diastereoselective formation of another product.

Thus, compounds ax-(5) and eq-(5) [see Scheme (III)] are diastereomers and eq-(5) is formed in a slightly lower but still

Table 1
Experimental details.

	(3)	(4)	ax-(5)	eq-(5)	(6)
Crystal data					
Chemical formula	$C_{14}H_{19}ClO_8$	$C_{15}H_{22}O_9$	$C_{13}H_{20}O_7$	$C_{13}H_{20}O_7$	$C_{14}H_{22}O_6$
Chemical formula weight	350.75	346.33	288.3	288.3	286.32
Cell setting, space group	Monoclinic, $P2_1/n$	Monoclinic, $P2_1/c$	Monoclinic, $P2_1/n$	Monoclinic, $P2_1/n$	Triclinic, $P\overline{1}$
a, b, c (Å)	8.117 (1), 8.5598 (7), 23.786 (3)	10.858 (3), 14.1170 (8), 11.519 (4)	11.498 (3), 8.4175 (8), 15.632 (4)	8.629 (6), 11.047 (7), 14.573 (4)	8.070 (2), 8.753 (2), 11.084 (3)
α, β, γ (°)	90, 98.19 (5), 90	90, 104.508 (10), 90	90, 111.47 (1), 90	90, 91.66 (1), 90	77.03 (2), 72.27 (2), 73.14 (2)
V (Å^3)	1635.8 (4)	1709.4 (8)	1408.0 (5)	1388.6 (14)	705.7 (3)
Z	4	4	4	4	2
D_x (Mg m^{-3})	1.424	1.346	1.36	1.379	1.347
Radiation type	Cu $K\alpha$	Cu $K\alpha$	Mo $K\alpha$	Cu $K\alpha$	Cu $K\alpha$
No. of reflections for cell parameters	25	25	25	25	25
θ range (°)	29.05–53.38	10.19–18.85	14.80–21.20	16.83–52.68	15.52–40.75
μ (mm^{-1})	2.431	0.959	0.111	0.953	0.878
Temperature (K)	293	293	293	293	293
Crystal form, colour	Irregular, colourless	Irregular, colourless	Irregular, colourless	Irregular, colourless	Irregular, colourless
Crystal size (mm)	0.40 × 0.40 × 0.20	0.70 × 0.40 × 0.30	0.50 × 0.50 × 0.40	0.6 × 0.5 × 0.3	0.60 × 0.50 × 0.36
Data collection					
Diffractometer	CAD-4	CAD-4	CAD-4	CAD-4	CAD-4
Data collection method	$\omega/2\theta$ scans	$\omega/2\theta$ scans	$\omega/2\theta$ scans	$\omega/2\theta$ scans	$\omega/2\theta$ scans
Absorption correction	Empirical	None	None	None	None
T_{min}	0.810	–	–	–	–
T_{max}	0.999	–	–	–	–
No. of measured, independent and observed reflections	3274, 3203, 3203	5250, 3070, 3070	4175, 3196, 3196	5792, 2782, 2782	2934, 2669, 2669
No. of observed reflections	32 741	5250	4175	5792	2934
Criterion for observed reflections	$F^2 > 0$	$F^2 > 0$	$F^2 > 0$	$F^2 > 0$	$F^2 > 0$
R_{int}	0.013	0.05	0.03	0.025	0.012
θ_{max} (°)	72.63	72.86	27.42	73.12	74.71
Range of h, k, l	$-10 \rightarrow h \rightarrow 8$ $0 \rightarrow k \rightarrow 10$ $0 \rightarrow l \rightarrow 27$	$-13 \rightarrow h \rightarrow 13$ $0 \rightarrow k \rightarrow 17$ $-14 \rightarrow l \rightarrow 14$	$-14 \rightarrow h \rightarrow 13$ $-7 \rightarrow k \rightarrow 10$ $0 \rightarrow l \rightarrow 20$	$-10 \rightarrow h \rightarrow 10$ $-13 \rightarrow k \rightarrow 13$ $0 \rightarrow l \rightarrow 18$	$-9 \rightarrow h \rightarrow 10$ $-9 \rightarrow k \rightarrow 10$ $0 \rightarrow l \rightarrow 13$
No. and frequency of standard reflections	3 every 400 reflections	3 every 400 reflections	3 every 400 reflections	3 every 400 reflections	3 every 400 reflections
Intensity decay (%)	9	2	1	5	2
Refinement					
Refinement on	F^2	F^2	F^2	F^2	F^2
$R[F^2>0]$, $wR(F^2)$, S	0.058, 0.091, 1.031	0.049, 0.064, 1.002	0.063, 0.064, 1.001	0.047, 0.063, 1	0.072, 0.075, 1.001
No. of reflections and parameters used in refinement	3203, 284	3070, 306	3196, 262	2782, 262	2669, 266
H-atom treatment	All H-atom parameters refined	All H-atom parameters refined	All H-atom parameters refined	All H-atom parameters refined	Mixed
Weighting scheme	$w = 1/[30\sigma^2(F^2)]$	$w = 1/[3.52\sigma^2(F^2)]$	$w = 1/[7.15\sigma^2(F^2)]$	$w = 1/[7.54\sigma^2(F^2)]$	$w = 1/[11.2\sigma^2(F^2)]$
$(\Delta/\sigma)_{max}$	0.0004	0.014	0.007	0.004	0.019
$\Delta\rho_{max}$, $\Delta\rho_{min}$ (e Å^{-3})	0.408, −0.498	0.215, −0.255	0.331, −0.252	0.272, −0.203	0.401, −0.362
Extinction method	None	Zachariasen	Zachariasen	Zachariasen	Zachariasen
Extinction coefficient	–	128 (3) × 10^2	221 (12) × 10^1	152 (4) × 10^1	72 (5) × 10^1

Computer programs used: *Xtal ADDREF*, *DIFDAT*, *SORTRF*, *CRYLSQ*, *BONDLA*, *CIFIO* (Hall *et al.*, 2000).

comparable yield (24%) than its axial isomer (31%). The formation of these compounds in similar amounts might either indicate that both diastereomers are of similar stability or, if this is not the case, that formation of the less stable isomer is kinetically favoured. To find an answer to this question, the structures of both isomers were first completely optimized at the Hartree–Fock level (HF). To obtain more reliable relative energies we used these optimized geometries in single point calculations not only including correlation corrections calculated by means of Møller–Plesset perturbation theory (Møller & Plesset, 1934; Hehre *et al.*, 1986; Szabo & Ostlund, 1996) to the second order (MP2), but also zero-point vibrational energy. Additional geometry optimizations were carried out at the B3LYP/6-31G* level of density functional theory (Lee *et al.*, 1988; Becke, 1988, 1993). The influence of the solvent on the relative stabilities of the isomers was estimated using an electrostatic model (*see below*).

Moreover, in order to find out why the addition of HCl to (2*b*) (Scheme I), exclusively resulted in one isomer with the Cl atom in an axial position, we applied the same levels of theory to calculate the relative energy of this compound [(3), Scheme (IV)] and its hypothetical isomer where the Cl atom occupies an equatorial position. As in the case of ax-(5) and eq-(5) the electrostatic contribution to the solvent effect was included in some of the calculations.

The measured structural parameters of all compounds under consideration are compared with data calculated at the HF/6-31G* and the B3LYP/6-31G* level of computational chemistry.

2. Methods

Diffraction data were collected at room temperature in the $\omega/2\theta$ mode on Enraf–Nonius CAD4 diffractometers equiped with graphite monochromators employing either Cu $K\alpha$ [λ = 1.54179 Å for (3), (4), ax-(5) and (6)] or Mo $K\alpha$ radiation [λ = 0.71069 Å for eq-(5)]. Reduction of the raw diffraction data of all the compounds involved a Lorentz–polarization correction, while an absorption correction has only been applied to the data set of chloro compound (3).[1] All structures were solved with direct methods as implemented in the *Xtal*3.7 package of crystallographic routines (Hall *et al.*, 2000), employing *GENSIN* (Hall & Subramanian, 2000) to generate structure-invariant relationships and *GENTAN* (Hall, 2000) for the general tangent phasing procedure. All hydrogen positions could be located in difference-Fourier maps and, except H122 of (6), were refined isotropically. The atomic scattering factors used in the calculations are those from *International Tables for X-ray Crystallography*, Vol. IV, Tables 2.2B and 2.3.1 (Cromer, 1989; Cromer & Waber, 1989). Refinement was on F^2 and included all reflections. Further details of the X-ray structure determinations[2] are collected in Table 1.

All quantum chemical calculations were performed using the *GAUSSIAN*94 suite of quantum chemical routines (Frisch *et al.*, 1995), running on a cluster of workstations at the Rechenzentrum der RWTH Aachen. Unconstrained geometry optimizations were carried out at the one-determinant (HF, Hartree–Fock) level of *ab initio* theory. Correlation corrections were then calculated employing Møller–Plesset perturbation theory to the second order (MP2) and HF/6-31G*-optimized structures. Additional calculations were performed with a density functional method (B3LYP), combining the three-parameter exchange potential of Becke (1988, 1993) with the correlation potential of Lee *et al.* (1988). All complete geometry optimizations were performed with the 6-31G* split-valence basis set (Ditchfield *et al.*, 1971; Hehre *et al.*, 1972; Hariharan & Pople, 1973, 1974), while additional calculations on model compounds have been performed with the 6–311++G** basis set.

3. Results and discussion

3.1. (1*RS*,3*RS*,4*SR*,5*SR*,7*SR*,8*SR*)-4-Acetyl-8-((1*SR*)-hydroxy)ethyl-1,3,5,7-tetramethyl-2,6,9,10-tetraoxatricyclo-[3.3.1.1^{3,8}]decane (6)

The synthesis and structure of (2*a*) [Scheme (I)] have been described recently (Thomas *et al.*, 1993; Simons, 1992). When this compound is reduced with $NaBH_4$ in ethanol (1*RS*,3*RS*,4*SR*,5*SR*,7*SR*,8*SR*)-4-acetyl-8-((1*SR*)-hydroxy)ethyl-1,3,5,7-tetramethyl-2,6,9,10-tetraoxatricyclo[3.3.1.1^{3,8}]decane (6) was obtained [Scheme (II)]

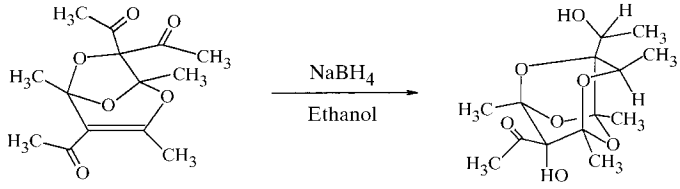

(2*a*) (II) (6)

besides derivatives of 2,4-diacetyl-3,5-dimethyl furan. Single crystals of sufficient quality for X-ray structure determination of (6) were obtained from an ether:pentane mixture (1:1). The structure of the molecule in the solid state is shown in Fig. 1.

3.2. 8-(Hydroxy)methyl-1,3,5,7-tetramethyl-2,6,9,10-tetraoxatricyclo[3.3.1.1^{3,8}]decane-4-carboxylic acid methyl ester [ax-(5) and eq-(5)]

Reduction of (2*b*) [*cf.* Scheme (I)] with $NaBH_4$ in ethanol resulted in similar amounts of two diastereomers of 8-(hydroxy)methyl-1,3,5,7-tetramethyl-2,6,9,10-tetroxatricyclo-[3.3.1.1^{3,8}]decane-4-carboxylic acid methyl ester [ax-(5) and eq-(5), see Scheme (III)].

[1] Comparison of the bond lengths derived from the corrected and uncorrected diffraction data of this compound (*cf.* Table 2) shows that the conclusions drawn regarding these structural parameters remain valid even if the absorption correction was omitted. If, however, this is the case for strongly absorbing (3), where the product of the median size of the crystal and the linear absorption coefficient amounts to 0.8, this should also be true for eq-(5), (6) and (4) where it is approximately 0.4.

[2] Supplementary data for this paper are available from the IUCr electronic archives (Reference: JZ0010). Services for accessing these data are described at the back of the journal.

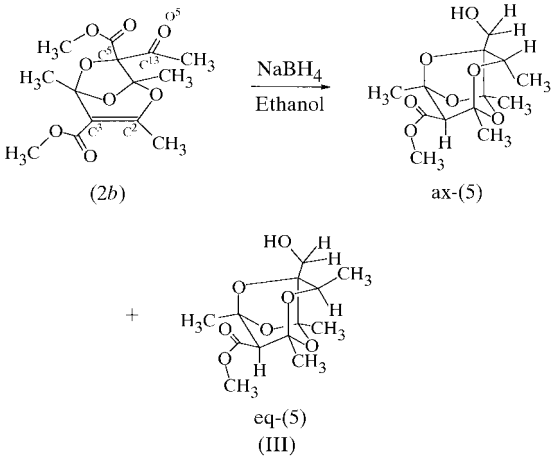

The formation of both diastereomers in comparable yields indicates that the attack of the hydride anion occurs with approximately equal probability from both sides of carbon C13 [(2*b*), see Scheme (III)]. It therefore appears that both the ester and the acetyl group at C5 are reduced simultaneously since the *exo* face is shielded effectively by the methoxy group in such reactions where the ester group remains intact. Thus, the addition of HCl to (2*b*) yields only one of the possible diastereomers (*see below*). Crystals of sufficient quality for X-ray structure determination were obtained from ether. The molecular structures are shown in Figs. 2 and 3, respectively.

The main structural difference between ax-(5) and eq-(5) is the orientation of the methyl group at C6 with respect to the six-membered ring defined by the C1, O7, C6, C5, C9 and O8 atoms. While this substituent occupies an equatorial position in eq-(5), it is oriented axially in ax-(5). The differences between the molecular structures of these isomers are so small that both compounds not only crystallize in cells with similar volumes, but also in the same space group.

3.2.1. Relative stability of ax-(5) and eq-(5). Taking into account possible repulsive interactions between an axial methyl group (C18) at C6 with those at C1 and C9, one intuitively predicts eq-(5) to be energetically more favourable than ax-(5). This assumption is supported by the results of our quantum chemical *ab initio* calculations (for the isolated molecules in the gas phase) in which the structures of both isomers were completely optimized at the HF/6-31G* level (Fig. 4).

Correlation corrections (MP2) and zero-point energies were then obtained in single-point calculations at HF-optimized geometries. The calculated normal frequencies showed that both structures are local minima. All computational results predict ax-(5) to be 15–16 kJ mol^{-1} higher in energy than its equatorial isomer (HF/6-31G*//HF/6-31G*: 15.0 kJ mol^{-1}; MP2/6-31G*//HF/6-31G*: 16.1 kJ mol^{-1}, ZPE+MP2/6-31G*//HF/6-31G*: 15.7 kJ mol^{-1}). A very similar value was obtained at the B3LYP/6-31G* level of density functional theory where complete geometry optimizations resulted in a relative energy of 14.9 kJ mol^{-1} in favour of eq-(5). Interestingly, with the 6-31G* basis set the energy difference between both isomers is almost independent of the inclusion of correlation and zero-point vibrational energy. Moreover, correction of the HF energies by inclusion of correlation energy obtained with the MP2 method slightly increases the energy difference, while in many cases the correlation energy favours the sterically more encumbered species and, therefore, reduces the energy difference.

The fact that in spite of this significant energy difference both isomers are obtained in comparable yields shows that the formation of the products is obviously determined by parameters other than the relative energy of the isolated molecules. Thus, one possibile explanation is that the formation of the axial isomer is favoured kinetically. However, it might also be that due to its higher dipole moment the axial isomer (HF/6-31G*: μ = 2.1 D) is stabilized more effectively in polar solvents (EtOH) than the equatorial diastereomer with a

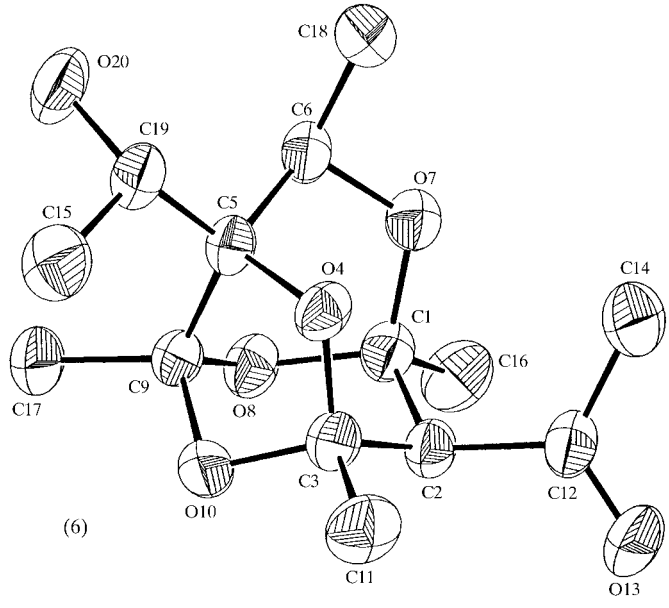

Figure 1
The molecular structure of (6) in the solid state (the numbering of atoms in the drawings is arbitrary and does not correspond to IUPAC rules).

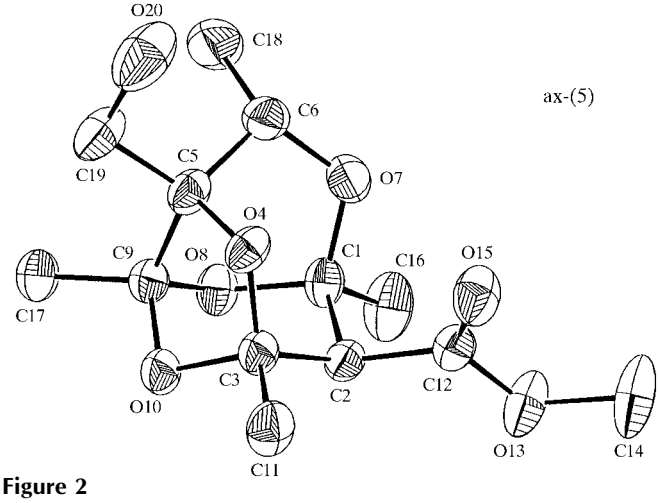

Figure 2
The molecular structure of ax-(5) in the solid state.

somewhat smaller dipole moment (HF/6-31G*: μ = 1.4 D) and thus a solvent effect accounts for the observed product distribution.

To substantiate this assumption we performed further single-point calculations in the presence of the solvent using the SCIPCM (*self-consistent isodensity polarized continuum*) model (Wiberg *et al.*, 1996). Employing a dielectric constant of ε = 25.8 (EtOH) and an isodensity value of 0.0004 a.u. we found that the stabilization of the solute due to electrostatic interaction with the solvent is indeed approximately 8 kJ mol^{-1} more effective for the axial isomer. Although this value is not sufficient to equalize the total energies of ax-(5) and eq-(5), it indicates that a more complete treatment of the solvent might result in comparable energies for both isomers.

3.3. (1*SR*,3*RS*,4*RS*,5*RS*,7*SR*,8*SR*)-7-Chloro-1,3,5,7-tetramethyl-2,6,9,10-tetraoxatricyclo[3.3.1.1^{3,8}]decane-2,6-dicarboxylic acid dimethylester (3)

Electrophilic addition of HCl in methylene chloride at 195 K to (2*b*) [*cf.* Scheme (IV)]

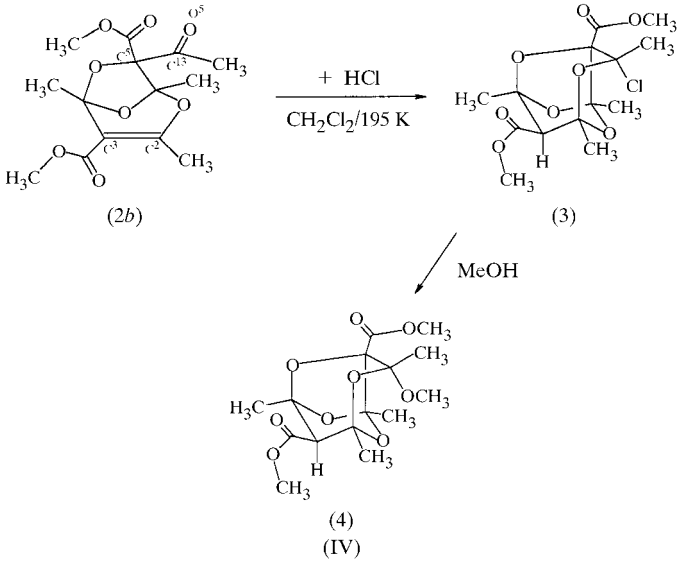

(2*b*) (3) (4)

(IV)

results in (1*SR*,3*RS*,4*RS*,5*RS*,7*SR*,8*SR*)-7-chloro-1,3,5,7-tetramethyl-2,6,9,10-tetraoxatricyclo[3.3.1.1^{3,8}]decane-2,6-dicarboxylic acid dimethylester (3) in a highly diastereoselective transanular reaction (diastereomeric excess, *d.e.*, > 96%). X-ray structure determination (Fig. 5) reveals that the Cl atom occupies an axial position of the six-membered ring defined by atoms C1, O7, C6, C5, C9 and O8. The initial step of the reaction [Scheme (V)]

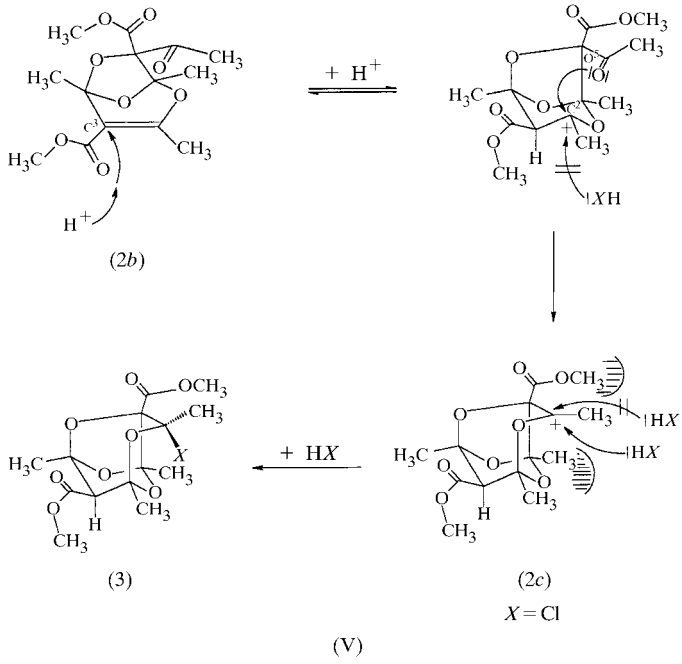

(2*b*) (3) (2*c*)

X = Cl

(V)

is most likely the attack of a proton at C3 of (2*b*). The O5 atom then adds to the cationic centre at C2, resulting in a transient carbenium ion (2*c*), which subsequently adds a chlorine anion to yield the observed product. Assuming a kinetically controlled reaction, exclusive formation of axial (3) might be explained by shielding of the exocyclic face of transient (2*c*) against the attack of the nucleophil by the methoxy group of the neighbouring ester substituent. This kinetically active shielding effect of the OMe group is supported by the experimental result that the addition of HCl to (2*d*), where the OMe group at C19 was replaced by the sterically less demanding methyl substituent, yields a 3:1 mixture of the *exo* and the *endo* product. The selectivity of the addition is further enhanced by an energetic preference of the axial orientation of the Cl atom as evidenced by the results of further *ab initio* calculations at the experimentally found ax-(3) and its hypothetical equatorial isomer eq-(3). The structures of both compounds were completely optimized at the HF/6-31G* level (*cf.* Fig. 6) and again correlation corrections and zero-point energies were obtained in single-point calculations at HF-optimized structures. Both structures turned out to be local minima. Additional calculations were carried out with the B3LYP/6-31G* method. At all levels of theory the axial isomer is somewhat more stable than the equatorial structure (HF/6-31G*//HF/6-31G*: 9.3 kJ mol^{-1}, MP2/6-31G*//HF/6-31G*: 11.1 kJ mol^{-1}, ZPE+MP2/6-31G*//HF/6-31G*: 11.3 kJ mol^{-1}, B3LYP/6-31G*//B3LYP/6-31G*: 9.5 kJ mol^{-1}). Since in this case the more stable isomer ax-(3) (HF/6-31G*: μ = 4.2 D; B3LYP/6-31G*: μ = 4.1 D) has the higher dipole moment than

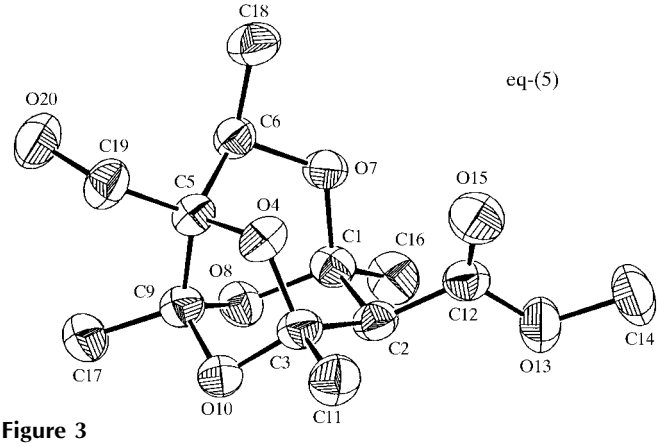

Figure 3
The molecular structure of eq-(5) in the solid state.

less stable eq-(3) (HF/6-31G*: μ = 2.8 D; B3LYP/6-31G*: μ = 2.6 D), the energy difference will be increased in the presence of a solvent. Thus, SCIPCM calculations (ε = 9.08, CH_2Cl_2; isodensity value: 0.0004 a.u.) revealed that stabilization owing to electrostatic interaction between the solvent and solute is indeed approximately 1.7 kJ mol^{-1} more stabilizing for ax-(3) than for its hypothetical equatorial isomer.

3.4. (1*SR*,3*RS*,4*RS*,5*RS*,7*SR*,8*SR*)-7-Methoxy-1,3,5,7-tetramethyl-2,6,9,10-tetraoxatricyclo[3.3.1.1^{3,8}]decane-2,6-dicarboxylic acid dimethylester (4)

When (3) was heated in MeOH for 5 min, (1*SR*,3*RS*,4*RS*,5*RS*,7*SR*,8*SR*)-7-methoxy-1,3,5,7-tetramethyl-2,6,9,10-tetraoxatricyclo[3.3.1.1^{3,8}]decane-2,6-dicarboxylic acid dimethylester (4) was obtained in the form of colourless crystals [*cf.* Scheme (IV)]. The structure of the molecule in the solid state is given in Fig. 7.

3.5. General structural considerations

A common structural feature of all five compounds is a rigid carbon–oxygen skeleton consisting of three fused rings of different size (*cf.* Fig. 8): the five-membered ring *R*1 (C3, O4, C5, C9, O10) and the six-membered rings *R*2 (C1, C2, C3, O10, C9, O8) and *R*3 (C1, O7, C6, C5, C9, O8). While *R*2 exists in its chair form in all five molecules, *R*3 can be described as a slightly twisted boat.

Although their packing in the crystal lattice is different, the calculated densities (Table 1) of the four C, H, O compounds are quite similar. While no classical intermolecular hydrogen bonds are present in the lattice of (4), the molecules of ax-(5), eq-(5) and (6) are crosslinked one-dimensionally by such bonds. In ax-(5) and its isomer eq-(5) the molecules are arranged in *zigzag* chains, extending parallel to the *bc* plane. In (6) the approximately linear chains are parallel to the

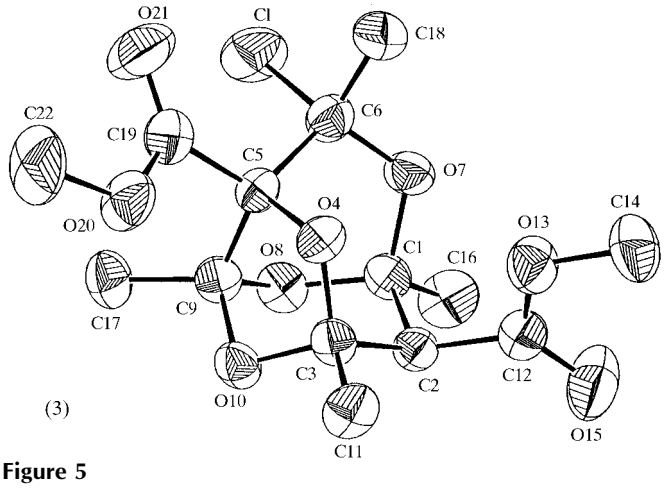

Figure 5
The molecular structure of (3) in the solid state.

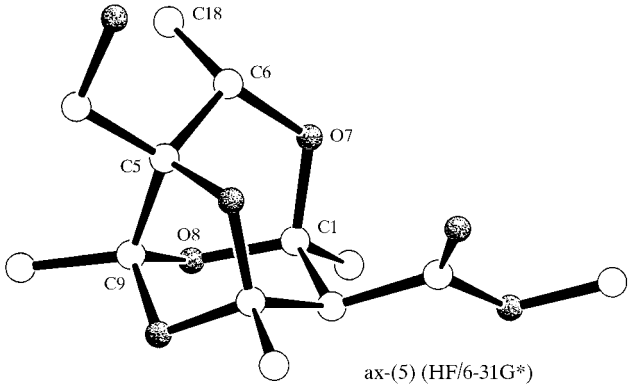

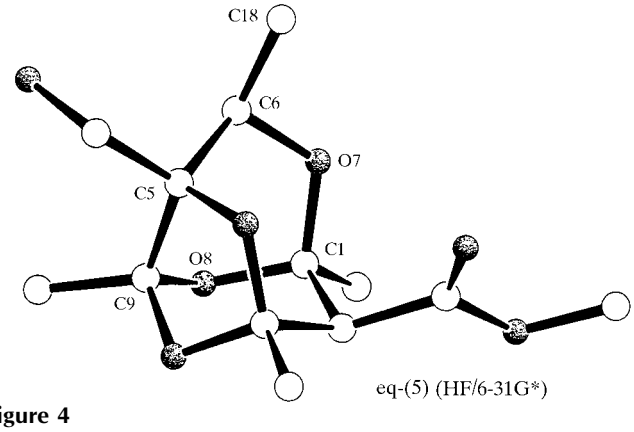

Figure 4
The molecular structures of ax-(5) and eq-(5) optimized at the HF/6-31G* level.

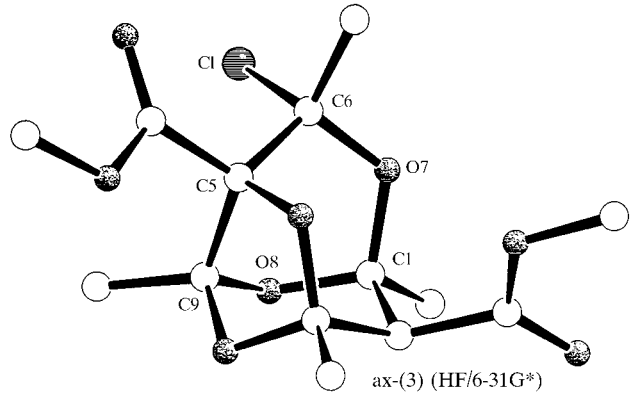

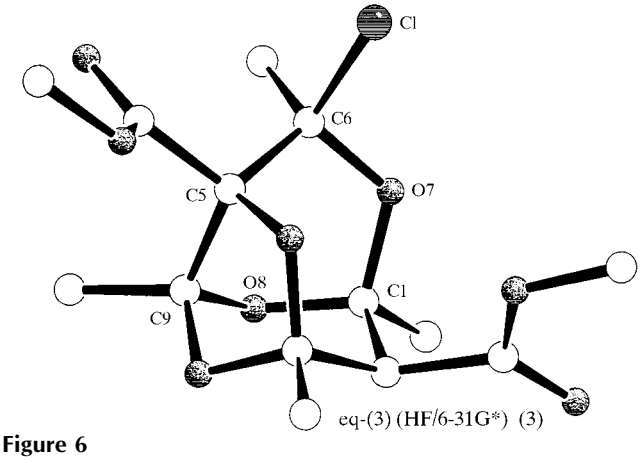

Figure 6
The molecular structures of ax-(3) and eq-(3) optimized at the HF/6-31G* level.

Table 2
Experimentally determined bond lengths (Å) and their standard deviations in ax-(5), eq-(5), (3), (4) and (6).

The numbers in italics are bond lengths obtained at the HF/6-31G* level. For the numbering of the atoms see Figs. 1–3, 5 and 7. An asterisk indicates that the calculated bond lengths are shorter than the experimental values in all five compounds (see text). The numbers in parentheses in the column headed (3) are bond lengths obtained from the diffraction data not corrected for absorption.

	ax-(5)	eq-(5)	(6)	(3)	(4)
C1—C2	1.557 (2) *1.566*	1.557 (2) *1.565*	1.557 (4) *1.553*	1.552 (3) [1.553 (4)] *1.559*	1.550 (2) *1.563*
C1—O7*	1.408 (2) *1.392*	1.415 (2) *1.396*	1.435 (4) *1.399*	1.440 (3) [1.441 (3)] *1.410*	1.424 (2) *1.404*
C1—O8*	1.423 (2) *1.399*	1.419 (2) *1.394*	1.412 (3) *1.395*	1.413 (3) [1.417 (4)] *1.389*	1.420 (2) *1.391*
C1—C16	1.510 (2) *1.516*	1.518 (2) *1.515*	1.484 (4) *1.514*	1.507 (4) [1.514 (5)] *1.513*	1.509 (3) *1.515*
C2—C3	1.538 (2) *1.546*	1.536 (2) *1.546*	1.536 (4) *1.543*	1.534 (3) [1.547 (4)] *1.544*	1.536 (3) *1.545*
C2—C12	1.512 (2) *1.519*	1.510 (2) *1.518*	1.514 (4) *1.531*	1.503 (4) [1.497 (5)] *1.520*	1.504 (3) *1.518*
C3—C11	1.511 (2) *1.510*	1.501 (2) *1.510*	1.520 (4) *1.510*	1.506 (4) [1.512 (5)] *1.508*	1.492 (3) *1.508*
C3—O4*	1.414 (2) *1.392*	1.423 (2) *1.396*	1.437 (4) *1.403*	1.438 (3) [1.431 (4)] *1.404*	1.426 (2) *1.398*
C3—O10*	1.429 (2) *1.403*	1.426 (2) *1.400*	1.423 (4) *1.398*	1.424 (3) [1.423 (4)] *1.396*	1.426 (2) *1.398*
C5—O4*	1.454 (2) *1.413*	1.440 (2) *1.412*	1.460 (3) *1.417*	1.428 (3) [1.429 (4)] *1.402*	1.426 (2) *1.396*
C5—C6	1.521 (2) *1.535*	1.519 (2) *1.534*	1.516 (4) *1.540*	1.540 (3) [1.543 (4)] *1.549*	1.548 (2) *1.547*
C5—C9	1.561 (3) *1.566*	1.555 (2) *1.565*	1.563 (4) *1.570*	1.577 (3) [1.565 (4)] *1.577*	1.570 (2) *1.574*
C5—C19	1.517 (3) *1.523*	1.537 (2) *1.527*	1.522 (3) *1.535*	1.536 (4) [1.550 (5)] *1.532*	1.533 (3) *1.535*
C6—O7*	1.441 (2) *1.419*	1.447 (2) *1.413*	1.438 (3) *1.414*	1.396 (3) [1.387 (4)] *1.381*	1.422 (2) *1.406*
C6—O24					1.407 (2) *1.383*
C6—C18	1.526 (3) *1.524*	1.497 (3) *1.520*	1.505 (6) *1.519*	1.512 (4) [1.514 (5)] *1.519*	1.508 (3) *1.522*
C6—Cl				1.849 (3) [1.857 (3)] *1.823*	
C9—O8*	1.423 (2) *1.395*	1.439 (2) *1.399*	1.433 (3) *1.403*	1.427 (3) [1.438(4)] *1.393*	1.418 (2) *1.393*
C9—O10*	1.419 (2) *1.389*	1.424 (2) *1.392*	1.429 (3) *1.392*	1.414 (3) [1.420 (4)] *1.387*	1.418 (2) *1.388*
C9—C17	1.504 (2) *1.511*	1.497 (3) *1.509*	1.510 (5) *1.511*	1.495 (4) [1.495 (5)] *1.509*	1.497 (3) *1.507*
C12—O13	1.335 (2) *1.327*	1.344 (2) *1.326*	1.194 (3) *1.195*	1.323 (3) [1.321 (4)] *1.317*	1.332 (2) *1.327*
C12═O15	1.189 (2) *1.186*	1.196 (2) *1.187*		1.198 (4) [1.195 (5)] *1.190*	1.191 (2) *1.186*
C14—O13	1.455 (3) *1.417*	1.443 (3) *1.417*		1.444 (4) [1.450 (5)] *1.419*	1.457 (4) *1.418*
C19—O20	1.406 (3) *1.399*	1.425 (2) *1.402*	1.450 (3) *1.407*	1.323 (3) [1.322 (4)] *1.317*	1.320 (2) *1.317*
C19—C15			1.519 (5) *1.526*		
C19═O21				1.190 (4) [1.178 (4)] *1.185*	1.173 (3) *1.185*
C22—O20				1.459 (6) [1.463 (8)] *1.419*	1.446 (3) *1.418*
C25—O24					1.434 (3) *1.401*

diagonal of the *ab* plane. Since no neutron data are available the exact positions of the bridging H atoms and, therefore, the relative strengths of the hydrogen bonds remain uncertain. However, the fact that the shortest intermolecular O···O distances are comparable in ax-(5) and (6) [2.810 (2) and 2.888 (3) Å], but significantly longer in eq-(5) [3.015 (2) Å], might indicate that the hydrogen bonds are somewhat weaker for the latter compound.

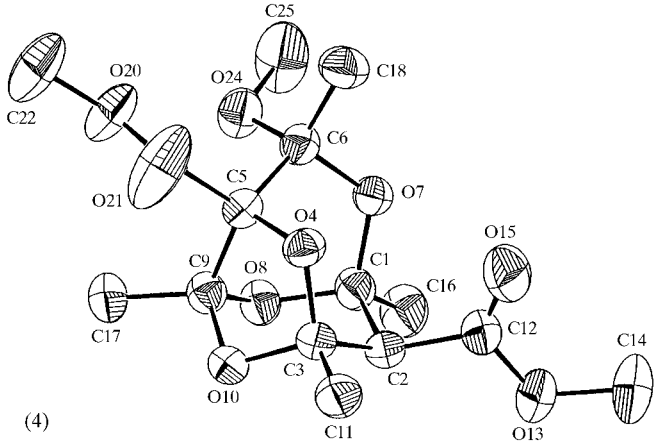

(4)

Figure 7
The molecular structure of (4) in the solid state.

In order to estimate the relative strengths of the hydrogen bonds we performed additional *ab initio* calculations on model systems. These model structures included only those heavy atoms which are involved in the hydrogen bonds plus their nearest neighbours [hydroxyl donor: C5, C19, O20; carbonyl acceptor: O15, C12, C2, O13, C14 for ax-(5) and eq-(5), hydroxyl donor: C5, C19, O20, C15; carbonyl acceptor: O13, C12, C14, C2 for (6)]. The free valencies of the C atoms have been saturated by H atoms calculated in idealized positions assuming C—H bond lengths of 1.09 Å. Keeping the coordinates of all other atoms constant we optimized the positions of the bridging H atoms at the MP2/6–311++G** level. The hydrogen bond strengths were then calculated as the differences between the total energies of the hydrogen-bonded complex and the sum of the total energies of its hydroxyl and carbonyl fragment. In this way we obtained hydrogen-bond energies of −22.2, −22.3 and −24.4 kJ mol^{-1}) for ax-(5), eq-(5) and (6). These values are within the range usually calculated for the hydrogen bonds

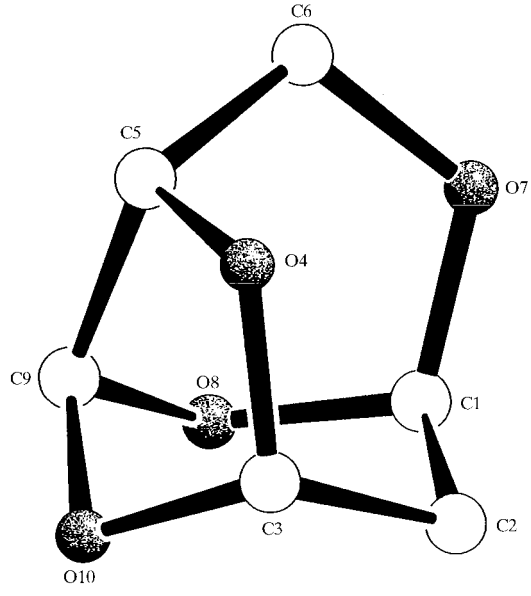

Figure 8
The three fused rings in (3), (4), ax-(5), eq-(5) and (6). *R*1: C3, O4, C5, C9, O10; *R*2: C1, C2, C3, O10, C9, O8; *R*3: C1, O7, C6, C5, C9, O8.

Table 3
Experimental average bond lengths (in Å) from (3), (4), ax-(5), eq-(5) and (6) (exp_{av}), average HF values (HF_{av}), corrected average HF values ($HF_{av,cor}$), together with the corresponding B3LYP/6-31G* average bond lengths ($B3LYP_{av}$).

	exp_{av}	HF_{av}	$HF_{av,cor}$	$B3LYP_{av}$
C1—O7	1.424 (3)	1.404 (7)	1.431 (7)	1.427 (9)
C1—O8	1.417 (2)	1.394 (3)	1.420 (3)	1.417 (5)
C3—O4	1.428 (3)	1.399 (4)	1.426 (4)	1.426 (6)
C5—O4	1.442 (2)	1.408 (8)	1.435 (8)	1.433 (8)
C6—O7	1.429 (2)	1.407 (13)	1.434 (13)	1.427 (18)
C9—O8	1.428 (2)	1.397 (4)	1.424 (4)	1.425 (5)
C9—O10	1.421 (2)	1.390 (2)	1.416 (2)	1.415 (2)
C3—O10	1.426 (3)	1.399 (2)	1.426 (2)	1.426 (3)
C6—C5	1.529 (3)	1.541 (6)		1.551 (7)
C5—C9	1.565 (3)	1.570 (5)		1.585 (6)
C1—C2	1.555 (3)	1.561 (5)		1.576 (5)
C2—C3	1.536 (3)	1.545 (1)		1.555 (1)

between alcohols and carbonyl compounds. Thus, at the MP2/6–311++G** level we obtained a hydrogen bond energy of -28.5 kJ mol^{-1} for the complex $(CH_3)_2C{=}O\cdots H{-}OCH_3$, where the structures of the complex and its components have been optimized completely. Moreover, taking into account possible uncertainties due to the use of partly optimized experimental structures, together with standard bonding parameters, we conclude that the hydrogen bonds in all three compounds are of comparable strength. It is interesting to note that the formation of the hydrogen bonds does not result in significantly different densities for ax-(5), eq-(5) and (6) compared with (4).

Calculated and uncorrected experimentally determined bond lengths cannot be compared to each other with a high level of accuracy (Cruickshank, 1956; Busing & Levy, 1964), however, a more qualitative discussion of some general trends is permissible. Usually, uncorrected interatomic distances, measured by means of standard X-ray diffraction methods, are *shorter* (Johnson, 1969; Johnson & Levy, 1989) than the corresponding bond lengths from *ab initio* calculations. It is, therefore, surprising that certain experimentally determined lengths of equivalent bonds in all five molecules significantly[3] *exceed* their calculated counterparts (Table 2).

This is the case for almost all C—O single bonds of the carbon–oxygen skeleton. Average values of the corresponding measured (exp_{av}) and HF-calculated bond lengths (HF_{av}) are given in columns two and three of Table 3. Several reasons might account for these striking differences. A careful analysis of the diffraction data revealed no indication for systematic errors. Moreover, we can exclude intermolecular forces (*i.e.* so-called crystal or lattice effects) as the origin of the differences between observed and calculated bond lengths. However, bond lengths calculated at the HF level are known to be too short in some cases. We therefore conclude that for the title compounds the chosen computational level (Hartree–Fock) is insufficient even for a rough and more qualitative

[3] We consider a difference between calculated and measured bond lengths significant if it exceeds the *threefold* estimated experimental standard deviation.

Table 4
Bond lengths in 2,6,9,10-tetraoxatricyclo[3.3.1.1^{3,8}]decane optimized at the HF/6-31G* and MP2/6-31G* level of *ab initio* theory (for numbering of atoms see Fig. 9).

	HF/6-31G*	MP2/6-31G*
C1—O7	1.394	1.422
C1—O8	1.400	1.426
C3—O4	1.396	1.422
C5—O4	1.411	1.437
C6—O7	1.405	1.429
C9—O8	1.392	1.421
C9—O10	1.386	1.413
C3—O10	1.400	1.430
C6—C5	1.517	1.516
C5—C9	1.548	1.549
C1—C2	1.539	1.527
C2—C3	1.525	1.522

comparison and that correlation energy has to be included in the geometry optimizations to obtain structural parameters which can be compared with the experimental values. Since the molecules under consideration turned out to be too large for complete geometry optimizations at the MP2 level, even when excitations of the core electrons were omitted, we have chosen the parent 2,6,9,10-tetraoxatricyclo[3.3.1.1^{3,8}]decane as a model compound (Fig. 9). Selected bond lengths of this compound calculated at the HF/6-31G* as well as at the MP2/6-31G* level are listed in Table 4. Comparison of the numbers in Tables 3 and 4 shows that in these cases, where the mean values of the experimentally determined bond lengths exceed the averaged HF/6-31G* results (Table 3), inclusion of correlation energy in the geometry optimizations increases the lengths of the corresponding bonds of our model compound

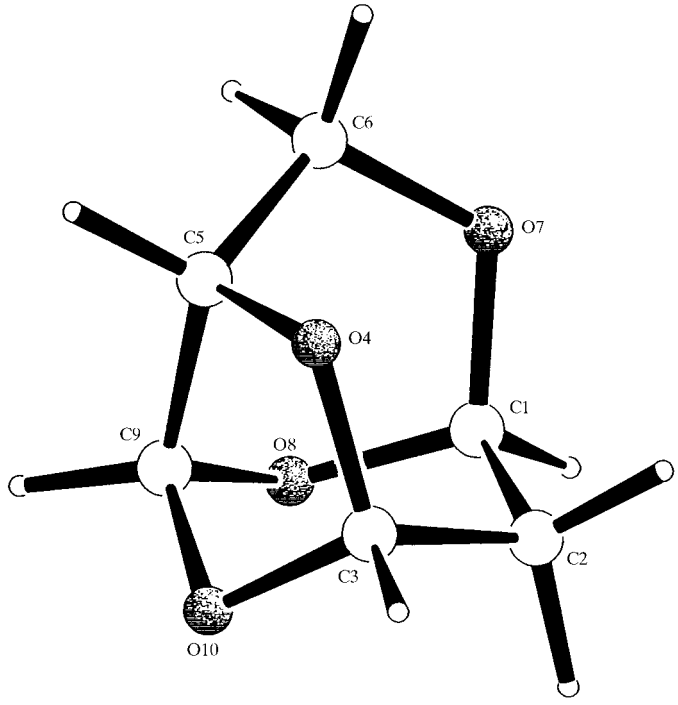

Figure 9
The structure of 2,6,9,10-tetraoxatricyclo[3.3.1.1^{3,8}]decane optimized at the MP2/6-31G* level.

by approximately 1.9% compared with the Hartree–Fock data (Table 4). In these cases, however, where, as to be expected, the experimental average values are smaller than their calculated counterparts, the effect of correlation energy on the calculated bond lengths is negligible. Applying such a 'correlation correction' of +1.9% to the average Hartree–Fock C—O bond lengths in Table 3 results in values ($HF_{av,cor}$) which overlap with the experimental values within their single standard deviations. The corrected bond lengths are also quite similar to the average B3LYP/6-31G* values ($B3LYP_{av}$, Table 3) calculated for the complete molecules.

One of us (GR) thanks the Crystallography Center of the University of Western Australia for generous financial support during his stay at the UWA. Moreover, financial support by the 'Fonds der Chemischen Industrie' is gratefully acknowledged. We thank Dr D. du Boulay of the Crystallography Center (UWA) and Dr T. Eifert of the Rechenzentrum der RWTH Aachen for their valuable technical support of our computational work.

References

Becke, A. D. (1988). *Phys. Rev. A*, **38**, 3098–3100.
Becke, A. D. (1993). *J. Chem. Phys.* **98**, 5648–5652.
Busing, W. R. & Levy, H. A. (1964). *Acta Cryst.* **17**, 142–146.
Cromer, D. T. (1989). *International Tables for X-ray Crystallography*, Vol. IV, edited by J. A. Ibers & W. C. Hamilton, pp. 149–150. Dordrecht: Kluwer Academic Publishers.
Cromer, D. T. & Waber, J. T. (1989). *International Tables for X-ray Crystallography*, Vol. IV, edited by J. A. Ibers & W. C. Hamilton, pp. 99–101. Dordrecht: Kluwer Academic Publishers.
Cruickshank, D. W. J. (1956). *Acta Cryst.* **9**, 757–758.
Ditchfield, R., Hehre, W. J. & Pople, J. A. (1971). *J. Chem. Phys.* **54**, 724–728.
Frisch, M. J., Trucks, G. W., Schlegel, H. B., Gill, P. M. W., Johnson, B. G., Robb, M. A., Cheeseman, J. R., Keith, T., Petersson, G. A., Montgomery, J. A., Raghavachari, K., Al-Laham, M. A., Zakrzewski, V. G., Ortiz, J. V., Foresman, J. B., Cioslowski, J., Stefanov, B. B., Nanayakkara, A., Challacombe, M., Peng, C. Y., Ayala, P. Y., Chen, W., Wong, M. W., Andres, J. L., Replogle, E. S., Gomperts, R., Martin, R. L., Fox, D. J., Binkley, J. S., Defrees, D. J., Baker, J., Stewart, J. P., Head-Gordon, M., Gonzalez, C. & Pople, J. A. (1995). *Gaussian*94, Revision D.4. Pittsburgh PA: Gaussian Inc.
Hall, S. R. (2000). *GENTAN, Xtal*3.7, edited by S. R. Hall, D. J. du Boulay and R. Olthof-Hazekamp. University of Western Australia, Australia.
Hall, S. R., du Boulay, D. J. & Olthof-Hazekamp, R. (2000). Editors. *Xtal*3.7. University of Western Australia, Australia.
Hall, S. R. & Subramanian, V. (2000). *GENSIN, Xtal*3.7, edited by S. R. Hall, D. J. du Boulay & R. Olthof-Hazekamp. University of Western Australia, Australia.
Hariharan, P. C. & Pople, J. A. (1973). *Theoret. Chim. Acta*, **28**, 213–222.
Hariharan, P. C. & Pople, J. A. (1974). *Mol. Phys.* **27**, 209–214.
Hehre, W. J., Ditchfield, R. & Pople, J. A. (1972). *J. Chem. Phys.* **56**, 2257–2261.
Hehre, W. J., Radom, L., von R. Schleyer, P. & Pople, J. A. (1986). *Ab Initio Molecular Orbital Theory*. New York: John Wiley and Sons.
Johnson, C. K. (1969). *Crystallographic Computing*. Proc. of the 1969 International Summer School on Crystallographic Computing Topic F: Analysis of Atomic Thermal Vibrations, pp. 220–226, edited by F. R. Ahmed, S. R. Hall and C. P. Huber. Copenhagen: Munksgaard.
Johnson, C. K. & Levy, H. A. (1989). *International Tables for X-ray Crystallography*, edited by J. A. Ibers and W. C. Hamilton, Vol. IV, pp. 312–336. Dordrecht: KluwerAcademic Publishers.
Lee, C., Yang, W. & Parr, R. G. (1988). *Phys. Rev. B*, **37**, 785–789.
Møller, Ch. & Plesset, M. S. (1934). *Phys. Rev.* **46**, 618–622.
Simons, J. (1992). Doctoral Thesis. Rheinisch-Westfälische Technische Hochschule Aachen, Germany.
Szabo, A. & Ostlund, N. S. (1996). *Modern Quantum Chemistry*. Mineola: Dover Publications Inc.
Thomas, H. G., Wellen, U., Simons, J. & Raabe, G. (1993). *Synthesis*, pp. 1113–1120.
Wiberg, K. B., Cajeston, H. & Keith, T. A. (1996). *J. Comput. Chem.* **17**, 185–190.